VERIZONA PUBLISHER
Publishing Your Ideas

www.verizonaonlinepublishing.com
Vol: 1, Issue: 1

Material Science and Engineering with Advanced Research

Mechanical, Optical and Barrier Properties of PLA-layered silicate Nanocomposites Coated with Organic Plasma Polymer Thin Films

Sylvie Ligot [1,2], Samira Benali [2*], Rindra Ramy-Ratiarison [2], Marius Murariu [2], Rony Snyders [1,3] and Philippe Dubois [2,3]

[1]Chimie des Interactions Plasma-Surface, Center of Innovation and Research in Materials & Polymers (CIRMAP), Université de Mons - UMONS, Place du Parc 23, B-7000 Mons, Belgium

[2]Service des Matériaux Polymères et Composites, Center of Innovation and Research in Materials & Polymers (CIRMAP), Université de Mons - UMONS, Place du Parc 23, B-7000 Mons, Belgium

[3]Materia Nova Research Center, 1 Avenue Copernic, 7000 Mons

***Corresponding Author:** Samira Benali, Service des Matériaux Polymères et Composites, Center of Innovation and Research in Materials & Polymers (CIRMAP), Université de Mons - UMONS, Place du Parc 23, B-7000 Mons, Belgium, Tel : +32-0-65-373477, Fax : +32-0-65-373484 ; Email: samira.benali@umons.ac.be

Article Type: Research, **Submission Date**: 18 March 2015, **Accepted Date:** 29 April 2015, **Published Date:** 15 May 2015.

Citation: Sylvie Ligot, Samira Benali, Rindra Ramy-Ratiarison, Marius Murariu, Rony Snyders, et al. (2015) Mechanical, Optical and Barrier Properties of PLA-layered silicate Nanocomposites Coated with Organic Plasma Polymer Thin Films. Mater. Sci. Eng. Adv. Res 1(1): 20-30. doi: https://doi.org/10.24218/msear.2015.04.

Abstract

In the frame of the efforts that are nowadays provided to develop new environmentally-friendly products as biosourced alternative to petrochemical polymers, we investigated in this work new PLA-based materials for packaging applications obtained by combining bulk and surface modifications of PLA substrates. Four PLA-based nanocomposites were prepared by adding organo-modified layered silicates (either Cloisite® 30B or Cloisite® 20A) and a nucleating agent, i.e. N,N'-ethylenebis-stearamide (EBS). The combination of EBS with CL30B led to very good nanofiller dispersion into PLA-clay nanocomposite while allowing, unlike neat PLA, to preserve the structural and thermal properties of PLA under plasma treatment. Based on this study, PLA/CL30B/EBS nanocomposites have been selected to investigate their surface modification that consisted in depositing on this substrate an organic barrier coating, i.e. an ethyl lactate plasma polymer film (ELPPF) synthesized by plasma polymerization of ethyl lactate. The PLA/CL30B/EBS-ELPPF system allowed increasing the tensile modulus from 3800 MPa (uncoated film) to 5200 MPa at high power plasma while preserving the ultimate mechanical properties. In addition, optical properties study showed that PLA/CL30B/EBS-ELPPF is also the best UV-B protective material while keeping a good transparency. Finally, the oxygen transmission rate was reduced by 53% with respect to neat PLA. All properties of final material are discussed as a function of the characteristics of PLA-clay nanocomposite substrate, of the ethyl lactate plasma polymer film (ELPPF) and of the substrate/plasma film interface.

Keywords: Polylactide, Layered silicate, Nanoclay, Plasma Polymer coating, Barrier, Morphology.

Introduction

Nearly all of the food and drink that we buy and then consume are packaged in some way. The main functions of food packaging are to protect and preserve the food, to maintain its quality and safety, and to reduce food waste. However, almost all plastic packaging are nowadays produced from fossil resources. These petrochemical-based plastics present important drawbacks that become more and more limiting in view of our modern world challenges. Among them, the most important are (i) unstable cost due to numerous factors affecting the price of crude oils, (ii) a strong emission of CO_2 during their production, and (iii) the extremely long degradation time generating plastic landfill issues [1]. To overcome, at least partly, these drawbacks, the use of the so-called "biobased polymers" is more and more considered. Currently packaging represents the largest application of biobased polymers, while following the growing of environmental concerns regarding the plastics disposal and sustainability, a further boom is expected. Among them, poly(lactic acid) (PLA)-based products are promising to reduce the environmental impact of plastic materials because in addition to the fact that they are biobased, they are also (bio)degradable following firstly the hydrolysis of the ester bonds that leads to successive reductions of molecular weights; finally soil microorganisms can digest the oligomer fragments to produce CO_2, H_2O, and biomass as end-products [2-4]. PLA is furthermore a good candidate for new developments because the physical and mechanical properties can be tailored through the polymer architecture while allowing the most common methods to process it [5,6].

Unfortunately, when considering packaging applications, PLA presents too low barrier properties against gases such as CO_2 and O_2 but also against water vapor, which represents a bigger problem in view of its sensitivity to moisture and the degradation mechanism by hydrolysis of the aliphatic polyester chain. High gas permeability of PLA strongly limits its use for packaging applications for food or electronic devices. Moreover, when considering semi-durable and long lifetime packaging products, the high water vapor permeability can lead to a too fast degradation of the materials. In order to widen the use of

PLA in packaging industry, it is therefore important to be able to reduce and to control the permeability of the package against water vapor and gases. Certainly, as a function of the foreseen application, it would be ideal to be able to tune the water vapor permeability and, as a consequence, the degradation rate of PLA. Indeed, if food packages may require a short lifetime (a few weeks), it is obvious that for semi-durable packaging, a longer one (a few years) is needed.

Since a decade, numerous researches have been developed in order to reduce the gas permeability of PLA. The topic is of high interest for both academic and industrial research. The barrier improvements were mainly obtained by modifying the bulk or by coating the surface of the polyester, by co-extrusion and realization of multilayer films, or using other techniques. Several bulk modifications of PLA have been reported in literature: (i) the blending of PLA with other polymers such as, among others, poly(glycolic acid) (PGA) or poly(methyl methacrylate) (PMMA),[7,8] (ii) the tuned isomeric ratio of the L and D enantiomer forms of the PLA's monomer,[6] and (iii) the incorporation of nano- and microfillers to the PLA matrix in order to synthesize PLA (nano)composites [9-13].

As it is well known, polymer nanocomposites are reinforced polymers produced by incorporating materials that have one or more dimensions on the nanometer scale (< 100 nm), such as layered silicates, carbon nanotubes, nanofibers, nanowhiskers, ultrafine layered titanate, zinc nanoxide or inorganic–organic nanohybrid systems [13-15]. Layered silicates clays, mainly montmorillonite, are the most commonly used nanomaterials in the plastics industry owing to their exceptionally high surface-to-volume ratio, availability and low cost [13]. In this field, Cloisite® products (supplied by Southern Clay Products, part of BYK Additives), which are organo-modified montmorillonite, have already been reported as very promising barrier nanoparticles [16,17]. As a consequence, Cloisite®30B and Cloisite®20A were considered in this work as barrier and impermeable nanofillers for the production of PLA nanocomposites. Additionally, since the permeability properties, through the diffusion gas process, are affected by the amount and size of crystals in the considered matrix, a nucleating agent (N,N'-ethylenebis-stearamide, hereinafter abbreviated as EBS) has also been incorporated into the PLA matrix.

On the other hand, as it is performed for most of the conventional polymers used in packaging, surface coating with a strong barrier layer has also investigated as an additional element to improve the global barrier properties of the material [18-21]. The most promising data have been reported for conventional inorganic coatings such as silicon oxide (SiO_x) and aluminum oxide (Al_2O_3). For example, it has been reported that Al_2O_3 coatings synthesized by atomic layer deposition reduce the oxygen transmission rate of PLA substrates of around 95 %. However, using this process, the temperature of the substrate rises too much increasing the crystallinity and rigidity of PLA. As a result, the PLA substrate becomes more brittle, which may lead to cracks in the polymer layer impairing the barrier properties [22,23]. SiO_x is another rather common coating used to improve the barrier properties of PLA. For example, Uemura *et al.* decreased by 50 % the water vapor permeation of PLA by using a stretched PLLA film covered by a SiO_x coating as synthesized by plasma polymerization of tetramethoxysilane [24]. However, this kind of barrier coatings does not allow to reduce enough the permeability to be competitive with respect to well-established petrochemical polymers and, moreover, the barrier efficiency cannot be modulated in the view of the targeted applications.

In this context, we have recently developed a new family of barrier coatings that would allow tuning the gas permeability of the package substrate and, in addition, that would respect the "green" feature of PLA [23,24]. These thin organic and cross-linked (bio) degradable barrier coatings have been synthesized by Plasma Enhanced Chemical Vapor Deposition (PECVD) and more precisely by plasma polymerization. Contrary to a conventional polymer, plasma polymer films are not characterized by repeating monomer units and exhibit an intrinsic cross-linked structure which grant them various advantages such as a flawless thin coating, good adhesion to the substrate, mechanical toughness, thermal stability, transparency, functional and barrier properties [25-27].

In our case, the plasma polymer coatings are synthesized by using a bio-based and biodegradable derivative of lactic acid, namely ethyl lactate. The synthesized coatings are therefore ethyl lactate plasma polymer films, ELPPF. In previous works, we reported the possibility to finely control the physicochemical properties of the ELPPF by modulating the experimental parameters. For example, by increasing the injected radiofrequency (RF) power in the plasma discharge, the ester function density in the ELPPF is reduced from 18 to 2 % and the cross-linking degree of the ELPPF increases by a factor 2 [28,29]. By using this deep control of the ELPPF synthesis, we expect to tune: (i) the diffusion rate of water vapor and other gases within the ELPPF by controlling the degree of cross-linking of the network; and (ii) the degradation rate of the ELPPF through the control of the ester bond density in the material.

In this work, we combine the mentioned bulk modifications and barrier coating developments in order to improve and tune the properties of PLA (Figure 1). To perform this study, four PLA-based nanocomposites and neat PLA as reference were synthesized and processed as films, in order to determine the optimal nanocomposite as substrate for ELPPF deposition by plasma polymerization. Then, the PLA-clay-ELPPF has been

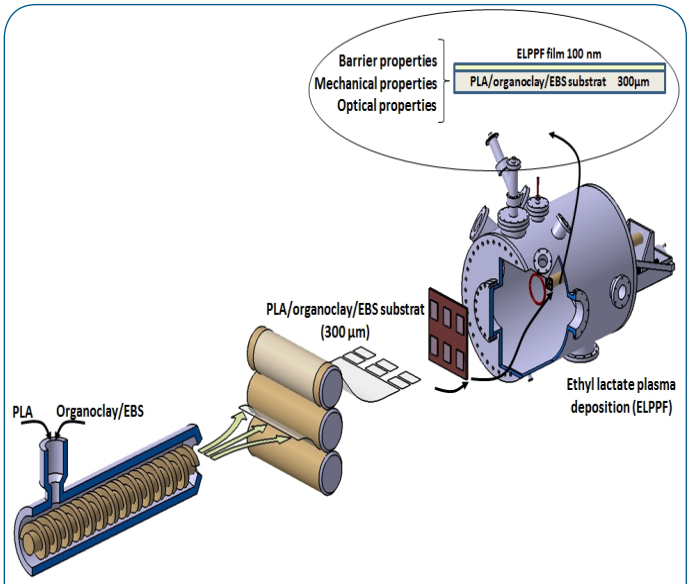

Figure 1: Overall strategy applied in the aim to improve and control the properties of PLA film

prepared and analyzed in terms of mechanical, optical and barrier properties. For this study, three values of the injected power used to grow the barrier coating were considered.

This combined approach should ultimately allow synthesizing PLA packaging films presenting new features and tunable degradation rate.

Experimental section

Materials

Poly(L,L-lactide) (PLA) is provided by NatureWorks LLC, grade (4032D) with $M_{n(PS)}$ = 119000 g/mol, index of polydispersity D = 2.0 defined by the ratio of the weight-average and the number-average molar masses (characterized by the authors from SEC analysis), D-isomer ~ 1.4 %; relative viscosity = 3.94; melt-flow index (MFI) = 7 g/cm^3 (210°C/2.16kg); residual monomer = 0.14 % (NatureWorks LLC informations). N,N'-ethylenebis(stearamide) (EBS) was provided by Aldrich while Cloisite®30B (CL30B) and Cloisite®20A (CL20A) are supplied by Southern Clay Products.

Table 1 summarizes the main characteristic parameters of the organo-modified layered silicates (OMLS). The PLA nanocomposites were obtained with 3 and 0.75 wt% of OMLS and EBS, respectively. The liquid precursor for the plasma polymer film synthesis, ethyl lactate, was supplied from Sigma Aldrich (≥99.0% purity).

Table 1: Main parameters of commercial organo-modified layered silicates studied in this work

Commercial name	Quaternary ammonium cations	d-spacing [a] (Å)	Organic content [b](wt%)
Cloisite®30B	methyl bis(2-hydroxyethyl)tallowalkyl ammonium[c]	18.4	28.4
Cloisite®20A	dimethyl di(hydrogenated tallowalkyl) ammonium[c]	24.2	29.2

[(a)]Assessed by XRD - [(b)]Assessed by TGA - (c)Tallowalkyl represents a mixture of linear alkyl chains containing approximately 65%C18, 30%C_{16}, and 5%C_{14}

Preparation of PLA-based nanocomposites

Before processing, PLA was dried overnight at 60°C in a convection oven. To minimize the water content for melt-blending with PLA, all additives were also dried in same conditions. The preparation of PLA-based nanocomposites and their processing by extrusion as films was performed in three steps. First, the dried granules of PLA and additives were mixed in a Rondol turbo-mixer (2000 rpm, 2 min). Second, PLA-based nanocomposites (with 3 wt% of OMLS and 0.75 wt% of EBS) were prepared by melt-compounding using a twin-screw extruder Leistritz ZSE 18 HP-40D (screw diameter (D) = 18 mm, L (length)/D ratio = 40) and the following conditions of processing: throughput = 1.5 kg/h, speed of screws = 100 rpm, extrusion temperatures around of 200°C, the temperature of molten polymer in the extrusion head before the extrusion of rods (for cooling and pelletizing) was about 185°C. For the sake of comparison, neat PLA was processed in similar conditions of melt-compounding. Third, the PLA-based nanocomposite pellets were dried overnight at 80°C in a convection oven to be extruded as films of about 300 µm-thick with a Brabender single screw extruder (D = 19 mm, L/D = 25) adapted with a extrusion die head (ribbon die of 100 mm wide, gap of 0.5 mm) and using for drawing a Univex flat film take-off unit as downstream equipment and having the temperature of the nip rolls of 60°C. After processing, all substrates were stored under controlled conditions (23°C, RH = 41 %) and were regularly characterized by DSC and TGA to attest the stability overtime of films used as substrates.

ELPPF coating synthesis

The ELPPF were synthesized on a disk of PLA of 5 cm of diameter. The deposition chamber consists of a cylindrical stainless steel vacuum chamber (35.5 cm in diameter and 86.5 cm in length) equipped with a rotary pump (Varian Triscroll 600) and a turbomolecular pump (Oerlikon Leybold Vacuum MAG W 600 iP/L) connected in series, allowing to reach a residual pressure of 6.6 x 10^{-4} Pa. The liquid precursor, ethyl lactate, is introduced in the chamber using a mass flow controller and an inlet system (Omicron) entirely heated at 343 K (container, tubes and connectors). During the process, the working pressure is accurately regulated by a throttle valve controlled by a capacitive gauge. The water-cooled copper coil (4.5 cm internal diameter and 0.7 cm thickness) is located in front of the substrate and connected to a RF power supply (13.56 MHz, Advanced Energy Cesar 1310) via a matching network (Advanced Energy VM1000A). The distance between the coil and the substrate is fixed at 13 cm. The substrates are introduced under vacuum through a load-lock system, and then transferred to the deposition chamber using a transfer stick.

ELPPF were synthesized at three different mean powers (P_{RF}): 30, 100 or 280 W. Due to technical limitation, it was impossible to get a stable continuous wave discharge at P_{RF} lower than 60 W. Therefore, pulsed mode signal was used to get steady plasma of 30 W by using a P_{peak} and an on-time fixed at 120 W and 0.25 ms, respectively. During the experiments, the working pressure and the precursor flow rate were fixed at 1.33 Pa and 5 sccm (standard cubic centimetre per minute), respectively.

Characterization

PLA solutions were prepared in $CHCl_3$ (2mg polymer/mL solvent). Molecular weight parameters (M_n, M_w and molar mass dispersity $Đ_M$) of pristine PLA were determined by SEC performed in $CHCl_3$ at 30°C using an Agilent liquid chromatograph equipped with an Agilent degasser, an isocratic HPLC pump (flowrate= 1mL min^{-1}), an Agilent autosampler (loop volume= 100 µL, solution concentration =2mg.mL^{-1}), an Agilent-DRI refractive index detector and three columns: a PL gel 5 µm guard column and two PL gel Mixed-B 5 µm columns (linear columns for separation of $M_{W(PS)}$ ranging from 200 to 4 × 10^5 g mol^{-1}). Polystyrene standards were used for calibration.

Thermal behaviours of PLA-based substrates were measured

by differential scanning calorimetry (DSC) using a DSC Q2000 from TA Instruments in nitrogen atmosphere. Samples (weight ~ 10 mg) were sealed in aluminium pans and placed in the DSC instrument previously calibrated with indium. Samples were heated from 0 to 200°C with a rate of 10°C/min. The glass transition temperature (T_g), cold crystallization temperature (T_c) and melting temperature (T_m), as well as the cold crystallization (ΔH_c) and melting (ΔH_m) enthalpies were measured on the first heating scan. The degree of crystallization (eq.1) was calculated using the expression:

$$\chi_c = \left(\frac{\Delta H_m - \Delta H_c}{\Delta H^0_m} \right) .100 \quad (1)$$

where ΔH_m and ΔH_c are the melting and the cold crystallization enthalpies, respectively, ΔH^0_m is the reference ΔH_m (93.0 J/g) for PLLA crystals having an infinite size and considered 100% crystalline [30].

The stress–strain curves of neat PLA and PLA-based nanocomposites were recorded at 20°C at a constant deformation rate of 1 mm/min with a Lloyd LR 10 K tensile tester using dumbbell-shaped specimens (ASTM 638 norm) obtained by the die cutting of 300 µm-thick films. All tensile data were determined based on the average of five independent measurements allowing calculation of error bars.

Transmission electronic microscopy (TEM) experiments were used to evaluate the dispersion of nanofillers in the PLA matrix and carried out using a JEOL 2100 apparatus operating at 200 kV. Scanning electronic microscopy (SEM) images were recorded in order to evaluate the surface defects of the neat PLA and PLA-based nanocomposites by using a Hitachi SU8020 instrument.

X-ray diffraction (XRD) measurements, used to characterize the nanoscale dispersion of the layered silicate, were performed by using a Panalytical Empryean in theta-2theta mode.

Water contact angles were measured in air by the sessile drop technique on a tensiometer (DSA 10-MK2) equipped with a microlitre syringe. From a minimum of four contact angle measurements with four drops of deionized water (10 µl), the average contact angle and the standard deviation were calculated on naked and coated PLA-based substrates.

The UV-Visible absorption spectra were obtained by using a Varian CARY 5G UV-VIS-NIR. The UV and visible beams are produced by deuterium and tungsten lamps, respectively. The percentage of transmission was measured in a wavelength range from 200 to 800 nm.

Sample name	EBS (wt%)	CL20A (wt%)	CL30B (wt%)
PLA	/	/	/
PLA/CL20A	/	3.00	/
PLA/CL20A/EBS	0.75	3.00	/
PLA/CL30B	/	/	3.00
PLA/CL30B/EBS	0.75	/	3.00

Table 2: Compositions of the PLA-based nanocomposites in term of weight percentage of inorganic for organo-clays and weight percentage of EBS. wt%

Transport property experiments were performed using the gas permeability tester PERME®VAC-VBS provided by Labthink® for calendered circular films. Testing is based on the differential pressure method to determine the gas transmission rate of films according to the GB/T 1038-2000 standards. Data were averaged on three measurements, carried out under controlled temperature (23°C). By using reference films provided by Labthink®, the relative error of Oxygen Transmission Rate (OTR ($cm^3/m^2.d.Pa$), where d is signifying day), was found to be less than 10%.

Results and Discussion

Choice of PLA-based nanocomposite substrates

Five proceeded PLA-based substrates (see Table 2) were characterized in terms of morphological properties and behaviour under plasma treatment. As mentioned, the accuracy of OMLS dosing in the extrusion experiments was confirmed in each PLA nanocomposite via thermal gravimetric analysis (TGA).

Morphological properties: The distribution and the dispersion of the nanofillers in the PLA matrix strongly influence the resulting nanocomposite properties. Indeed, it has been reported that the transparency, the global mechanical behavior and the barrier properties can be strongly affected on the quality of dispersion and the nature of the considered nanofillers and matrices [31]. Since, XRD in conjunction with TEM are the usual methods used to characterize the nanoscale dispersion [32], Figure 2 and Figure 3 show the XRD diffractograms and the TEM images, respectively, of the PLA-based nanocomposites (PLA/CL30B, PLA/CL30B/EBS, PLA/CL20A and PLA/CL20A/EBS)

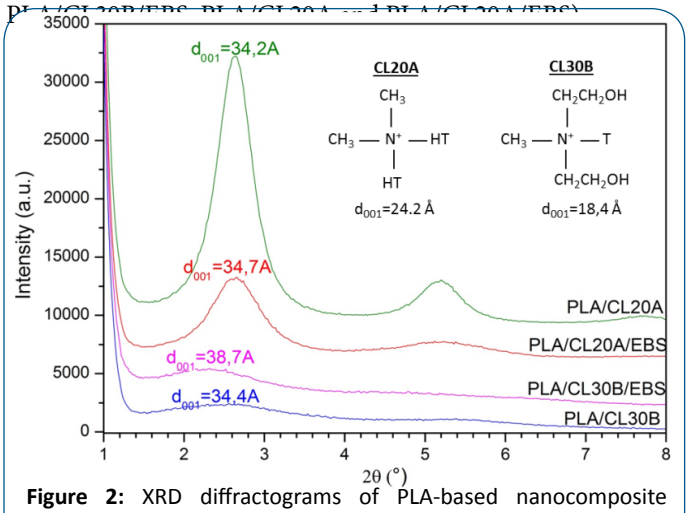

Figure 2: XRD diffractograms of PLA-based nanocomposite substrates

All PLA-based nanocomposites have one or two diffraction peaks of different intensity related to the nature of the organo-modified clay and corresponding to d_{001} and d_{002} planes, composition and structure of the nanocomposites. Indeed, according to the intercalated morphology, the repetitive multilayer structure is well preserved allowing the diffraction of the crystalline phases of nanoclays. In addition, the intercalation of the polymer chains between silicate layers increases the interlayer distance. Conversely, in exfoliated structure, the repetitive multilayer structure is lost leading to the absence of peaks. Based on the Bragg's law, the angle of diffraction and the interlayer distance are inversely proportional, thus a shift of the diffraction peak towards lower angle values is recorded when the interlayer

distance increases [33]. This shift in the lower range of 2-theta angle, accompanied by an important broadening and decreasing in intensity, is observed for CL30B in comparison to CL20A and highlights consequently more delamination and/or the better intercalation of the polymer chains between CL30B [34] than CL20A sheets. This assumption is supported by the measurements of the interlayer distances (d_{001}) in the nanocomposites (see Figure 2) since the latter increases with respect to initial d_{001} of OMLS, by 86 and 41% by adding CL30B and CL20A, respectively.

To investigate the size and spatial distribution of the intercalated or exfoliated clay platelets, XRD measurements have been complemented with TEM analyses of the four PLA-based nanocomposites. Figure 3 shows selected TEM pictures obtained at low and high magnifications, having the scale bar respectively at 1 µm (Figure 3a) and 100 nm (Figure 3b).

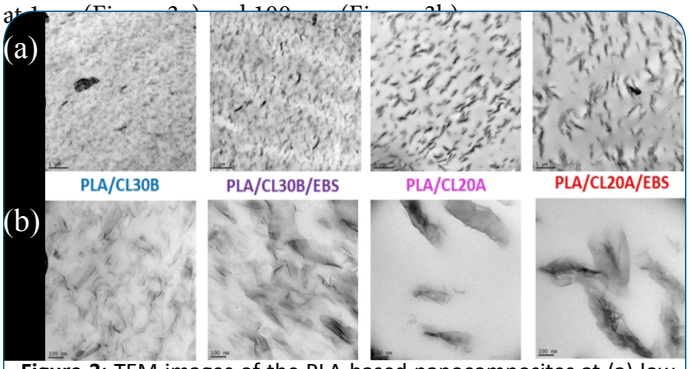

Figure 3: TEM images of the PLA-based nanocomposites at (a) low magnification (scale bar of 1 µm) and (b) at high magnification (scale bar of 100 nm)

As expected, the average clay size and related size distribution are of importance on the mechanical properties of the related nanocomposites. Their effects have been already reported and discussed in details for PLA/organoclay nanocomposites [35-37] and it is out of the scope of this contribution to discuss them again here. Clearly and based on our previous study [16,38], the TEM images shown in Figure 3 are in perfect line with previously reported data and will allow to highlight any possible effect of EBS on the quality and extent of organoclay distribution and dispersion within the PLA matrix.

Indeed, with few exceptions connected to presence of rare clusters, the TEM images confirm that blending CL20A with PLA matrix leads to nanocomposites showing a specific intercalated morphology, while PLA/CL30B shows advanced exfoliated structures [16]. This dissimilarity in nanocomposite structure has been explained by the chemical difference between the alkylammonium cations used to modify CL30B and CL20A. Indeed, as shown in Figure 2, the organic modifier of CL30B is an ammonium cation surrounded by two hydroxyl groups and one unsaturated long alkyl chain. The two hydroxyl groups can react (or interact) [39,40] with the C=O moieties of the ester functions present in the PLA backbone leading to good physicochemical affinity between the organic modifier and the polymer matrix, while the long alkyl involves more available space for the intercalation of the polymer chains. Both contribute by consequence to the exfoliation process. At the opposite, the organic modifier of CL20A has no polar groups such as hydroxyl and even if it has an initial d-spacing higher than those of CL30B (24.2Å compared to 18.4Å, respectively) due to presence of two long alkyl chains per ammonium head and a pronounced hydrophobicity, the penetration of the aliphatic polyester between clay layers and the increase in the gallery spacing is limited to some extent, behavior ascribed to a lower affinity of this OMLS for the PLA matrix. Furthermore, it was reported in the literature that a high degree of miscibility between modifier and matrix will provide a larger driving force for silicate platelet exfoliation and stacked clay sheets separation. The solubility parameters of PLA are closer to those of the organo-modifier used in CL30B, which suggests higher miscibility and compatibility of CL30B with the polyester matrix [41].

In addition, we can see that EBS is also well dispersed in the PLA matrix allowing a weak improvement of the clay dispersion that is more evident in the case of PLA/CL30B/EBS sample. For instance, as seen in Figure 2, d_{001} was increased (with more than 4Å) in the nanocomposites containing both EBS and CL30B nanofiller with respect to the nanocomposite PLA/CL30B (d_{001} of above 34Å). The good dispersion of EBS in PLLA matrix has already been reported by Xing *et al.* by means of SEM and TEM analyses [42]. Based on these morphological results, the PLA/CL30B/EBS substrate has been selected for coating/treatment with ELPPF.

PLA and PLA/CL30B/EBS substrate behaviour under plasma treatment

During the plasma polymerization process, the PLA and PLA/CL30B/EBS are bombarded by energetic electrons, ions and photons, which induce chemical rearrangements, ablation reactions and surface activations [43-45]. These phenomena lead usually to an increase of the substrate temperature, strongly dependent on the experimental parameters. For example, Thiry *et al.* has reported a substrate temperature reaching 100°C for high power conditions [46]. As the T_g of the five PLA-based substrates is around 61°C, it is necessary to guarantee that the substrate structure is preserved during the plasma polymerization. If the temperature increases further and exceeds T_c, PLA-based could even crystallize during the deposition process.

Visual tests and DSC analyses were consequently performed in order to determine the influence of the plasma treatment on the morphology of the substrates.

Pictures of the PLA and PLA/CL30B/EBS substrates were taken before and after the plasma deposition occurring for 3.5 min (Figure 4). Apparently none of the sample has suffered from damages and remains exactly similar even in term of visual transparency.

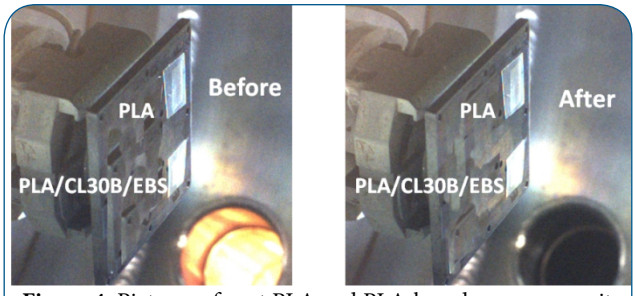

Figure 4: Pictures of neat PLA and PLA-based nanocomposites substrates before and after plasma treatment (280 W - 10 mTorr - 5 sccm) for 3.5 minutes

In order to more precisely study the influence of the plasma process on the PLA-based substrates, DSC analyses were recorded before and after the ethyl lactate plasma treatment (Figure 5).

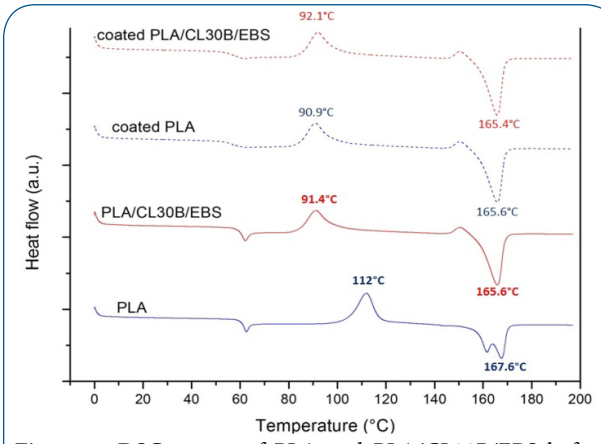

Figure 5: DSC curves of PLA and PLA/CL30B/EBS before and after plasma polymer deposition by using hard plasma condition (280 W- 10 mTorr - 5 sccm) for 3.5 min.

When coated, the T_C of neat PLA is significantly decreased from 112 to 91°C and the percentage of crystallinity is increased from 3.7 to 18.6 %. Conversely, after deposition, PLA/CL30/EBS preserves its T_C, T_m and crystallinity percentage around 91°C, 165°C and 15 %, respectively. This shows also that by heating the substrate, the plasma process leads to the crystallization of the neat PLA substrate even in 3.5 minutes in the α' form as depicted by the small exothermic peak at 150°C prior the melting peak, which is often ascribed to α'-crystal transformation into the α one [47]. In addition, whatever the considered substrates, the plasma process modifies the peak related to T_g [47]. Indeed, the glass transition of uncoated substrates is joined by enthalpy relaxation meaning that the inter- and intra-chain displacements are allowed. At the opposite, the coated substrates show only glass transition with absence of relaxation of polyester chain segment [9].

and neat PLA coated with the same deposition parameters. Due to technical limitation of the GPC analysis, the molar masses of the PLA-based nanocomposites cannot be determined. As reported In Tab. 3, the molar mass (M_n) decreases from 1.13 10^5 to 7.88 10^4 g/mol revealing the effective degradation of the polymer chains caused by the plasma deposition process.

Finally, this short study shows that the thermal properties of the PLA/CL30B/EBS substrate do not seem to be modified by the plasma treatment at the opposite of the neat PLA substrate. It is assumed that the PLA matrix in nanocomposite will be less degraded by plasma likely due to the presence of nanofiller and higher crystallinity conferred by a synergy between organoclays and EBS as very recently reported by Murariu *et al* [48].

Properties of plasma-coated PLA nanocomposite film (PLA/CL30B/EBS-ELPPF)

Since the foreseen applications are mainly in the packaging field, the generated coated PLA nanocomposite substrate, called PLA/CL30B/EBS-ELPPF is studied in terms of mechanical, barrier and optical properties.

Mechanical properties: For most of practical applications the mechanical resistance of plasma polymer films is also a critical parameter limiting their use at larger scale. Specifically in packaging applications, the durability of the coatings through adequate mechanical properties is a critical requirement. Metal oxide-based barrier coatings such as SiO_x or Al_2O_3 are usually used in the packaging field. However, these coatings have the drawback to reduce the resistance at break or to lead to crack propagations when the material is twisted or deformed by the regular use of the package [22,23]. In this work, organic plasma polymer films were used in order to improve the mechanical compatibility with the PLA-based substrates since the reduced modulus of ELPPF is significantly lower than the one of SiO_x thin

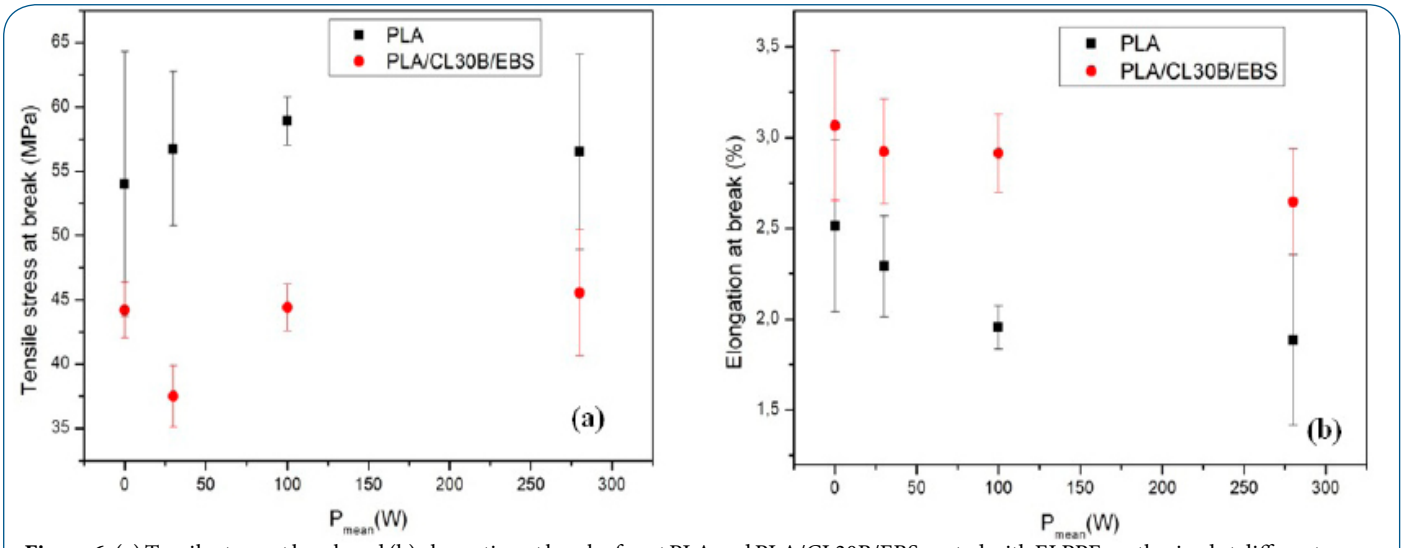

Figure 6: (a) Tensile stress at break and (b) elongation at break of neat PLA and PLA/CL30B/EBS coated with ELPPF synthesized at different powers

However, the bombardments of ions and photons on the polymeric substrates can affect their thermal properties. Indeed, the energetic species can break PLA macromolecules leading to shorter chains which rearrange themselves. This may lead to higher chain mobility and densification. In order to support this hypothesis, gel permeation chromatography (GPC) measurements were performed on PLA pellet, neat PLA substrate coating (35 GPa) [49]. In order to highlight the influence of the ELPPF on the mechanical properties of substrates, the tensile modulus, and the elongation at break of the PLA/CL30B/EBS-ELPPF system have been determined by tensile testing. Figure 6 and Figure 7 show the mechanical data of neat PLA and PLA/CL30B/EBS coated by ELPPF synthesized at P_{mean} = 30, 100 or 280 W.

The tensile stress at break (Figure 6a) remains in the short ranges of 55 to 60 MPa and 38 to 45 MPa when ELPPF is deposited on PLA and PLA/CL30B/EBS substrates, respectively. We can also see that the elongation at break (Figure 6b) decreases weakly when the power used to synthesize ELPPF increases. Indeed the elongation at break decreases from around 3 to 2.5 and from 2.5 to 2 % for neat PLA and PLA/CL30B/EBS substrates, respectively. Finally, the tensile modulus (Figure 7) is relatively constant (between 4000 and 4300 MPa) for neat PLA while a more significant increase from 3800 to 5200 MPa is observed when the ELPPF is deposited on PLA/CL30B/EBS. This increase is not surprising since the coatings are less and less ductile as the power increases. However, additional SEC measurements (Table 3) revealed that the PLA chains are degraded during the plasma treatment. This reduction of the PLA chain length could counterbalance the increase of the reduced modulus of the coated substrates and explain the constant modulus of the coated neat PLA substrates.

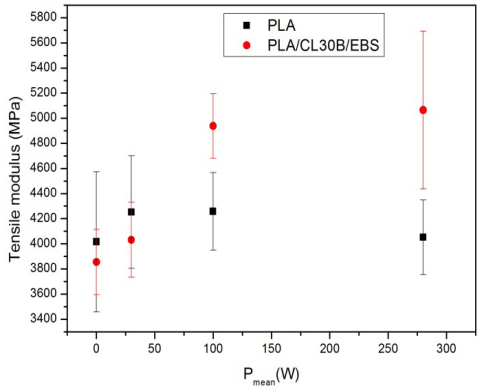

Figure 7: Tensile modulus of neat PLA and PLA/CL30B/EBS coated with ELPPF synthesized at different powers

Table 3: Number-average molar masses of PLA pellet, neat PLA substrate and coated-(neat) PLA substrate

Sample	M_n (g/mol)
PLA pellet	$1.19\ 10^5$
Neat PLA substrate	$1.13\ 10^5$
Coated-PLA substrate	$7.88\ 10^4$

Except the slight increase observed for the tensile modulus, these data reveal globally a weak influence of the coating on the tensile properties of the synthesized materials. This could be explained by the low thickness of the coating (100 nm) with respect to the much thicker substrate (300 µm). The mechanical properties of the coated material are therefore mainly related to the intrinsic properties of the considered substrate. As far as the modulus is concerned, the high level of the ELPPF cross-linking density is more likely responsible for the observed rigidity. Based on nanoindentation tests, we previously reported that the cross-linking degree of the ELPPF increases with the injected power and that a high level of cross-linking degree leads to reduce significantly the plastic contributions inducing to a global improvement of the mechanical performance in terms of wear and fracture resistance, hardness and self-healing capabilities [50].

Altogether, these data reveal that the mechanical properties of the coated substrates are improved in certain conditions by the presence of the ELPFF. Based on these data, depositing a coating synthesized at high power allows enhancing the mechanical performance of the system.

In packaging applications, the transmission of visible and ultraviolet light are important parameters to preserve and protect products until they reach the consumer as well as to get an attractive transparent package. It is consequently interesting to determine the influence of the substrate-clay based nanocomposite and ELPPF on the UV and visible transmission curves of the neat PLA-coated ELPPF and PLA/CL30B/EBS-coated ELPPF synthesized at different powers (Figure 8 and Table 4).

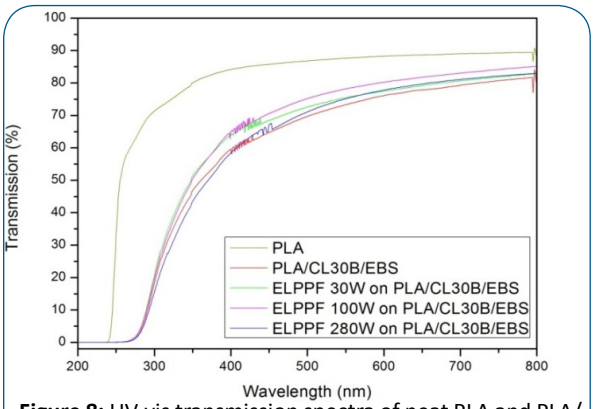

Figure 8: UV-vis transmission spectra of neat PLA and PLA/CL30B/EBS coated with ELPPF as synthesized at different powers

We can see that the PLA/CL30B/EBS-ELPPF offers an efficient barrier behaviour to UV-B as only around 15% of the light is transmitted, at higher plasma power, with regards to 71 % in case of neat PLA.

In the visible range (400-700 nm), each wavelength causes a particular sensation of color as the eye is not equally sensitive to light emitted at all wavelength. According to ASTM-D1746-03, the transparency of plastic sheeting is defined as the transmission of visible light in the short range of 540-560 nm. The measurement of the transmission percentage at 550 nm reveals that all substrates are transparent with around 87 % for the neat PLA that show the highest transmittance, around 75% transmittance for the PLA/CL30B/EBS-ELPPF samples and around 73% transmittance for just PLA/CL30B/EBS substrate (Table 4). The literature allows linking the transparency to higher exfoliation degree of clays [51-53].

Table 4: UV-vis transmittance at selected wavelengths (300 and 550 nm) of neat PLA and PLA/CL30B/EBS coated with ELPPF as synthesized at different powers

Substrate	Transmission of UV (300 nm) (%)	Transmission of visible light (550 nm) (%)
PLA	71.3	87.6
PLA/CL30B/EBS	18.3	73.3
ELPPF 30W ON PLA/CL30B/EBS	20.7	75.4
ELPPF 100W ON PLA/CL30B/EBS	19.7	78.2
ELPPF 280W ON PLA/CL30B/EBS	15.5	75.1

Indeed, the nanocomposites could be more transparent due to the changes of the particle size and spacing. As an example, when the nanofiller was not very well dispersed, Petersson et al have reported a drop of the visible light transmission from 86% (neat PLA) to 29% when 5 wt-% bentonite, another clay mineral is added to PLA matrix [54]. On the other hand, the results with ELPPF coating were expected based on the reported good transparency of plasma polymer films awarding them to be used in optical applications [45]. For example, optically transparent plasma polymer films were synthesized by Tien et al. and Couderc et al. from hexamethyldisiloxane (HMDSO) and hydrocarbonate precursors, respectively [55,56].

A more detailed analysis of the results allows to attribute these optical behaviours mainly to the PLA/CL30B/EBS substrate. For example, the transparency (measured at 550 nm) remains stable around 75 % whatever P_{mean} while, the transmission of UV-B light at 300 nm, which is strongly reduced by the addition of CL30B/EBS, is even lower for high power prepared ELPFF.

Barrier properties: The oxygen transmission rates of neat PLA and PLA/CL30B/EBS substrates coated with ELPPF were measured as a function of the injected power used to synthesize the ELPPF (P_{mean} = 30, 100 or 280W) (Figure 9). The coatings and the substrates were 100 nm and 300 µm thick, respectively.

The addition of CL30B/EBS reduces the OTR values around 53 %. The higher barrier efficiency obtained with PLA/CL30B/EBS may be explained by the fine dispersion of nanofiller and quality of the nanocomposite. The improvement of the barrier properties by using organo-modified clays and especially CL30B has been already reported in the literature [15, 48, 49]. For example, Zenkiew *et al.* have reduced the OTR of 40% by adding 5 wt% of CL30B and Bhatia *et al.* have synthesized a ternary nanocomposite PLA/PBS/CL30B showing an oxygen permeability 26 % less than neat PLA [48, 49]. This behavior is explained by the layered morphology of the clay nanoparticles and the exfoliated configuration. Indeed, high aspect ratio and dispersion of the nanoclays in the considered matrix increases the effective diffusion path length by forcing penetrant molecules on a "tortuous path" and is consequently preferred from a barrier property standpoint [50].

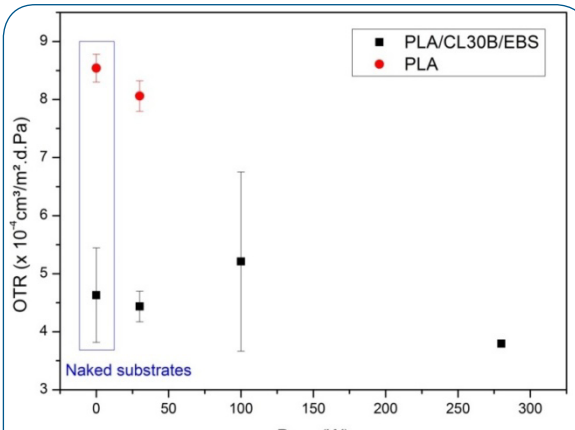

Figure 9: Influence of the power used to synthesize ELPPF on the OTR of the neat PLA and coated PLA/CL30B/EBS substrates

The observed set of data (Figure 9) reveals a slight influence of the plasma polymer on the barrier properties of the material. This influence is somewhat higher for high P_{mean} prepared ELPPF, i.e., 280 W. This behavior could be explained considering that the permeation of molecules through polymers occurs in two stages: (i) the dissolution of the permeant in the polymer, characterized by the sorption coefficient (S) and (ii) the diffusion of the dissolved permeant characterized by the diffusion coefficient (D). The former is mainly depending on the chemical affinity between the molecules and the polymer while the latter is function of the diffusion path of the molecules through the polymer.

It has been shown that for low power, the ELPPF are slightly cross-linked and contain much more ester functions, which result in polar and hydrophilic surfaces [28,29]. As a consequence, there is a good affinity between the polar groups at the surface of the coating and the oxygen molecules, which could increase the sorption coefficient and limit the barrier efficiency of the ELPPF. On the opposite, the ELPPF prepared at high power are strongly cross-linked and contain much less polar groups[28,29]. This should have the consequence to decrease the OTR and the diffusion pathway of oxygen molecules through. However, these coatings are also harder leading to mechanical mismatches between the coating and the substrate. Indeed, nanoindentation data reported in a previous work revealed that the elastic modulus of the ELPPF prepared at high power is about 9 GPa while the elastic modulus of the conventional PLA is around 3 - 4 GPa [50]. These mechanical differences likely generate local stress and may lead to cracks in ELPPF limiting the barrier efficiency, while some local degradation of the substrate can be also for discussion.

In order to support these hypotheses, the surface properties, i.e., the hydrophilicity and the surface defects have been evaluated for ELPPF synthesized for P_{mean} = 30, 100 and 280 W and deposited on neat PLA and PLA/CL30B/EBS. The measurements of the water contact angles (Figure 10) show that covering PLA-based substrates with ELPPF has as direct consequence and increases the hydrophilicity. However, as the power used to deposit ELPPF increases, the hydrophobicity increases. This supports a part of our understanding.

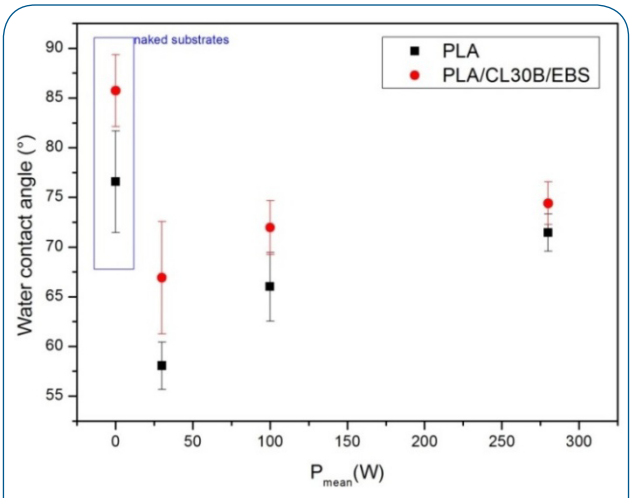

Figure 10: Water contact angle measurements of ELPPF deposited on neat PLA and PLA/CL30B/EBS substrates

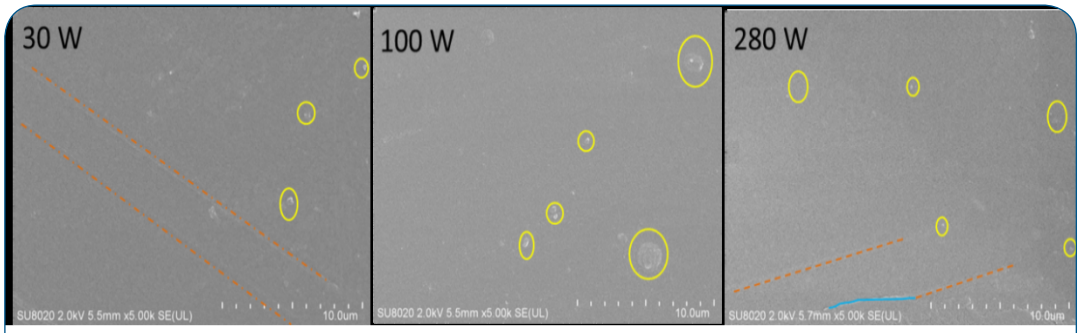

Figure 11: SEM images of ELPPF synthesized at different powers and deposited on PLA/CL30B/EBS

On the other hand, SEM images of the microstructure of the ELPPF surfaces were acquired in order to observe the presence of possible surface defects (Figure 11). As a reference, the SEM image of the uncoated PLA/CL30B/EBS substrate is shown in Figure 12.

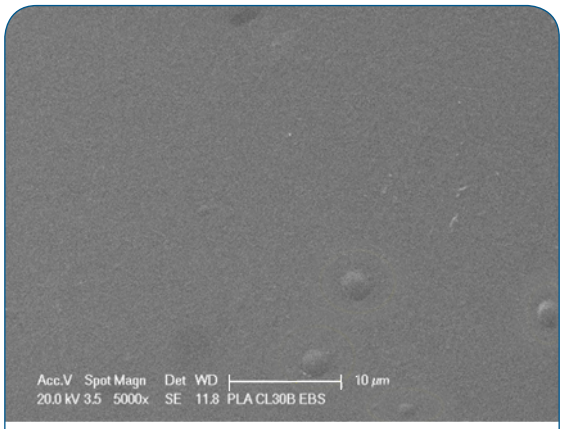

Figure 12: SEM image of the surface of the non coated PLA/CL30B/EBS substrate

We can see that whatever the power used to synthesize the ELPPF, defects are observed such as bumps, scratches or cracks as highlighted by yellow circle, orange line and blue line, respectively. Based on the SEM image of the uncoated PLA/CL30B/EBS substrate, the numerous bumps observed at the surface of the ELPPF could be related to the initial defects present at the surface of the substrate. However, Figure 11 also reveals the presence of microscratches and microcracks, mainly at the surface of the 280W-ELPPF. These results support the hypothesis of internal stress in ELPPF synthesized at higher power and the low resistance to crack propagations. This behavior has been indeed predicted by the high H/E_r ratio – where H is the hardness and E_r is the reduced Young's modulus- determined by nanoindentation tests in our previous paper [29]. Such a kind of phenomenon has already been reported, for example, for metal oxide coatings deposited on polymeric substrates. Chatham *et al.* demonstrated that the reduction in oxygen permeation due to the coatings is limited by transport through coating defects (e.g., pinholes, grain boundaries or microcracks) [57].

In conclusion, it is worth pointing out that globally by combining nanofillers and ELPPF, the OTR value of the PLA materials has been reduced by more than two times, which appears to be a promising result particularly in the field of packaging applications.

Conclusion

Neat PLA, and PLA-based nanocomposites prepared using commercially organo-modified clays (Cloisite®20A and Cloisite®30B) and nucleating agent (EBS) were studied in order to select the best substrate in the view of the deposition of an organic barrier layer obtained by plasma polymerization.

The morphological study shows that PLA/CL30B/EBS presents the best dispersion of the clay nanoplatelets with a relatively good degree of exfoliation. According to these data, PLA/CL30B/EBS was considered as a promising material for the deposition of the ethyl lactate plasma polymer coating. The key-characteristics of PLA/CL30B/EBS-ELPPF were studied in terms of mechanical, optical and barrier properties and compared to neat PLA. The tensile tests and optical characterizations reveal that the enhanced mechanical properties could be attributed in addition to the ELPPF coating and that the obtained PLA/CL30B/EBS-ELPPF material preserves the transparency and UV blocker properties.

Concerning the barrier properties of ELPPF, if the plasma polymer film does not affect significantly the oxygen permeability, this study allows to highlight the need to control the cross-linking degree of ELPPF while avoiding the induced crack propagation at high power. When deposited on PLA/CL30B/EBS, our data reveal a decrease of 53 % of the OTR with respect to PLA reference, corresponding to an oxygen transmission rate of 4.5 10^{-4} cm^3/m^2.d.Pa for the ELPPF synthesized at 280 W.

Both bulk modification at the nanoscale and the use of ethyl lactate plasma coating as barrier layer are promising ways for an improvement of the barrier properties of PLA. If it is still necessary to optimize the system, this work highlights the possibility for further modifying PLA using combined techniques in view of packaging applications.

Acknowledgments

Authors from the University of Mons acknowledge the Belgian Government through the « Pôle d'Attraction Interuniversitaire » (PAI, P07/34, "Plasma-Surface Interaction", Ψ and PAI P7/05 "Functional Supramolecular Systems") and the Wallonia Region through the program of excellence "EVERWALL". Authors are grateful to Yoann Paint and Lisa Dangreau for assistance in realization of analyses. Sylvie Ligot is grateful to the « Fonds pour la Formation à la Recherche dans l'Industrie et dans l'Agriculture » (F.R.I.A.) for her financial support.

References

1. Slomkowski S, Penczek S, Duda A. Polylactides—an overview. Polym Adv Technol. 2014; 25(5):436-447. doi: 10.1002/pat.3281.
2. Kale G, Auras R, Singh SP, Narayan R. Biodegradability of Polylactide Bottles in Real and Simulated Composting Conditions. Polym Test. 2007; 26(8):1049-1061. doi:10.1016/j.polymertesting.2007.07.006.
3. Maharana T, Mohanty B, Negi Y. Melt–solid polycondensation of lactic acid and its biodegradability. Progress in Polymer Science. 2009; 34(1):99-124. doi:10.1016/j.progpolymsci.2008.10.001.
4. Ray SS, Yamada K, Okamoto M, Ueda K. New polylactide-layered silicate nanocomposites. 2. Concurrent improvements of material properties, biodegradability and melt rheology. Polymer. 2003; 44(3):857-866. doi:10.1016/S0032-3861(02)00818-2.
5. Stevens E. Green Plastics - An Introduction to the New Science of Biodegradable Plastics. USA: Princeton University Press; 2002. 238 p.
6. Auras R, Harte B, Selke S. An overview of polylactides as packaging materials. Macromolecular bioscience. 2004; 4(9):835-864. doi: 10.1002/mabi.200400043.
7. Samuel C, Raquez J-M, Dubois P. PLLA/PMMA blends: A shear-induced miscibility with tunable morphologies and properties? Polymer. 2013; 54(15):3931-3939. doi:10.1016/j.polymer.2013.05.021.
8. Auras R, Lim L-T, Selke S, Tsuji H, editors. Poly(lactic acid) : Synthesis, Structures, Properties, Processing, and Application. New Jersey: Wiley & sons; 2010. 528 p.
9. Courgneau C, Domenek S, Lebossé R, Guinault A, Avérous L, Ducruet V. Effect of crystallization on barrier properties of formulated polylactide. Polymer International. 2012; 61(2):180-189. doi: 10.1002/pi.3167.
10. Lemmouchi Y, Murariu M, Santos AMD, Amass AJ, Schacht E, Dubois P. Plasticization of poly(lactide) with blends of tributyl citrate and low molecular weight poly(d,l-lactide)-b-poly(ethylene glycol) copolymers. Eur Polym J. 2009; 45(10):2839-2848. doi:10.1016/j.eurpolymj.2009.07.006.
11. Yasuda H, Hsu T. Plasma polymerization investigated by the comparison of hydrocarbons and perfluorocarbons. Surf Sci. 1978; 76(1):9. doi:10.1016/0039-6028(78)90077-8.
12. Paul MA, Delcourt C, Alexandre M, Degée P, Monteverde F, Dubois P. Polylactide/montmorillonite nanocomposites: study of the hydrolytic degradation. Polymer Degradation and Stability. 2005; 87(3):535-542. doi:10.1016/j.polymdegradstab.2004.10.011.
13. Sanchez-Garcia MD, Lopez-Rubio A, Lagaron JM. Natural micro and nanobiocomposites with enhanced barrier properties and novel functionalities for food biopackaging applications. Trends in Food Science & Technology. 2010; 21(11):528-536. doi:10.1016/j.tifs.2010.07.008.
14. Sinha Ray S, Bousmina M. Biodegradable polymers and their layered silicate nanocomposites: In greening the 21st century materials world. Progress in Materials Science. 2005; 50(8):962-1079. doi:10.1016/j.pmatsci.2005.05.002.
15. Pantani R, Gorrasi G, Vigliotta G, Murariu M, Dubois P. PLA-ZnO nanocomposite films: Water vapor barrier properties and specific end-use characteristics. European Polymer Journal. 2013; 49(11):3471-3482. doi:10.1016/j.eurpolymj.2013.08.005.
16. Paul M-A, Alexandre M, Degée P, Henrist C, Rulmont A, Dubois P. New nanocomposite materials based on plasticized poly(l-lactide) and organo-modified montmorillonites: thermal and morphological study. Polymer. 2003; 44(2):443-450. doi:10.1016/S0032-3861(02)00778-4.
17. Rhim J-W, Hong S-I, Ha C-S. Tensile, water vapor barrier and antimicrobial properties of PLA/nanoclay composite films. LWT - Food Science and Technology. 2009; 42(2):612-617. doi:10.1016/j.lwt.2008.02.015.
18. Jiang J, Benter M, Taboryski R, Bechgaard K. Oxygen barrier coating deposited by novel plasma-enhanced chemical vapor deposition. J Appl Polym Sci. 2010; 115(5):2767-2772. doi: 10.1002/app.30222.
19. Lugscheider E, Bärwulf S, Riester M, Hilgers H. Magnetron sputtered titanium nitride thin films on thermoplastic polymers. Surf Coat Technol. 1999; 116–119(0):1172-1178. doi:10.1016/S0257-8972(99)00157-7.
20. Chim H, Ong JL, Schantz J-T, Hutmacher DW, Agrawal CM. Efficacy of glow discharge gas plasma treatment as a surface modification process for three-dimensional poly (D,L-lactide) scaffolds. J Biomed Mater Res A. 2003; 65(3):327-335.
21. Iotti M, Fabbri P, Messori M, Pilati F, Fava P. Organic–Inorganic Hybrid Coatings for the Modification of Barrier Properties of Poly(lactic acid) Films for Food Packaging Applications. J Polym Environ. 2009; 17(1):10-19. doi: 10.1007/s10924-009-0120-4.
22. Hirvikorpi T, Vähä-Nissi M, Nikkola J, Harlin A, Karppinen M. Thin Al2O3 barrier coatings onto temperature-sensitive packaging materials by atomic layer deposition. Surf Coat Technol. 2011; 205(21–22):5088-5092. doi:10.1016/j.surfcoat.2011.05.017.
23. Hirvikorpi T, Vähä-Nissi M, Mustonen T, Iiskola E, Karppinen M. Atomic layer deposited aluminum oxide barrier coatings for packaging materials. Thin Solid Films. 2010; 518(10):2654-2658. doi:10.1016/j.tsf.2009.08.025.
24. Uemura Y, Maetsuru Y-S, Fujita T, Yoshida M, Hatate Y, Yamada K. The effect of coatings formed by low temperature tetramethoxysilane plasma treatment on water-vapor permeability of poly(L-lactic acid) film. Korean J Chem Eng. 2006; 23(1):144-147. doi: 10.1007/BF02705706.
25. Yasuda H. Plasma Polymerization. Orlando: Academic Press Inc; 1985. 432 p.
26. Biederman H. Plasma Polymer Films. London: Imperial College Press; 2004. 386 p.
27. Inagaki N. Plasma Surface Modification and Plasma Polymerization. Pennsylvania: Technomic publication; 1996. 265 p.
28. Ligot S, Renaux F, Denis L, Cossement D, Nuns N, Dubois P, et al. Experimental Study of the Plasma Polymerization of Ethyl Lactate. Plasma Processes and Polymers. 2013; 10(11):999-1009. doi: 10.1002/ppap.201300025.
29. Ligot S, Guillaume M, Gerbaux P, Thiry D, Renaux F, Cornil J, et al. Combining Mass Spectrometry Diagnostic and Density Functional Theory Calculations for a Better Understanding of the Plasma Polymerization of Ethyl Lactate. J Phys Chem B. 2014; 118(15):4201-4211. doi: 10.1021/jp411244x.
30. Fukada E. Piezoelectricity of biopolymers. Biorheology. 1995; 32(6):593-609.
31. Paul DR, Robeson LM. Polymer nanotechnology: Nanocomposites. Polymer. 2008;49(15):3187-3204. doi:10.1016/j.polymer.2008.04.017.
32. Morgan AB, Gilman JW. Characterization of polymer-layered silicate (clay) nanocomposites by transmission electron microscopy and X-ray diffraction: A comparative study. J Appl Polym Sci. 2003; 87(8):1329-1338. doi: 10.1002/app.11884.
33. Eberhart J-P. Analyse structurale et chimique des matériaux. Paris: Dunod; 1997. 614 p.

34. Zaidi L, Bruzaud S, Bourmaud A, Médéric P, Kaci M, Grohens Y. Relationship between structure and rheological, mechanical and thermal properties of polylactide/Cloisite 30B nanocomposites. J Appl Polym Sci. 2010; 116(3):1357-1365. doi: 10.1002/app.31655.

35. Heinz H, Koerner H, Anderson KL, Vaia RA, Farmer BL. Force Field for Mica-Type Silicates and Dynamics of Octadecylammonium Chains Grafted to Montmorillonite. Chemistry of Materials. 2005; 17(23):5658-5669. doi: 10.1021/cm0509328.

36. Saito T, Okamoto M. Polypropylene-based nano-composite formation: Delamination of organically modified layered filler via solid-state processing. Polymer. 2010; 51(18):4238-4242. doi:10.1016/j.polymer.2010.06.049.

37. Kajino M, Saito T, Okamoto M, Sato H, Ozaki Y. Nonisothermal order–disorder phase transition of alkylammonium ions in nanoconfined space. Applied Clay Science. 2010; 48(1):73-80. doi:10.1016/j.clay.2009.11.025.

38. Paul M-A, Delcourt C, Alexandre M, Degée P, Monteverde F, Rulmont A, et al. (Plasticized) Polylactide/(Organo-)Clay Nanocomposites by in situ Intercalative Polymerization. Macromol Chem Phys. 2005; 206(4):484-498. doi: 10.1002/macp.200400324.

39. Bordes P, Pollet E, Avérous L. Nano-biocomposites: biodegradable polyester/nanoclay systems. Prog Polym Sci. 2009; 34(2):125-155. doi:10.1016/j.progpolymsci.2008.10.002.

40. Pluta M, Galeski A, Alexandre M, Paul MA, Dubois P. Polylactide/montmorillonite nanocomposites and microcomposites prepared by melt blending: Structure and some physical properties. J Appl Polym Sci. 2002; 86(6):1497-1506. doi: 10.1002/app.11309.

41. Krikorian V, Pochan DJ. Poly (L-lactic acid)/layered silicate nanocomposite: fabrication, characterization, and properties. Chemistry of Materials. 2003; 15(22):4317-4324. doi: 10.1021/cm034369+.

42. Xing Q, Zhang X, Dong X, Liu G, Wang D. Low-molecular weight aliphatic amides as nucleating agents for poly (L-lactic acid): Conformation variation induced crystallization enhancement. Polymer. 2012; 53(11):2306-2314. doi:10.1016/j.polymer.2012.03.034.

43. Friedrich J. The Plasma Chemistry of Polymer Surfaces. Weinheim: Wiley-VCH Verlag & Co; 2012. 275 p.

44. Chan CM, Ko TM, Hiraoka H. Polymer surface modification by plasmas and photons. Surf Sci Rep. 1996; 24(1–2):1-54. doi:10.1016/0167-5729(96)80003-3.

45. D'Agostino R. Plasma Deposition, Treatment, and Etching of Polymers. San Diego: Academic Press; 1990.

46. Thiry D, Aparicio FJ, Britun N, Snyders R. Concomitant effects of the substrate temperature and the plasma chemistry on the chemical properties of propanethiol plasma polymer prepared by ICP discharges. Surf Coat Technol. 2014; 241(0):2-7. doi:10.1016/j.surfcoat.2013.10.063.

47. Pan P, Zhu B, Kai W, Dong T, Inoue Y. Polymorphic transition in disordered poly (L-lactide) crystals induced by annealing at elevated temperatures. Macromolecules. 2008; 41(12):4296-4304. doi: 10.1021/ma800343g.

48. Murariu M, Dechief A-L, Ramy-Ratiarison R, Paint Y, Raquez J-M, Dubois P. Recent advances in production of poly (lactic acid) (PLA) nanocomposites: a versatile-method to tune crystallization properties of PLA. Nanocomposites. 2014; 1(2):1-12. doi: http://dx.doi.org/10.1179/2055033214Y.0000000008.

49. Trivedi R, Cech V. Mechanical properties of plasma polymer film evaluated by conventional and alternative nanoindentation techniques. Surf Coat Technol. 2010; 205(Suppl 1):S286-S289. doi:10.1016/j.surfcoat.2010.08.002.

50. Ligot S, Bousser E, Cossement D, Klemberg-Sapieha J, Viville P, Dubois P, et al. Correlation Between Mechanical Properties and Cross-Linking Degree of Ethyl Lactate Plasma Polymer Films. Plasma Process Polym. 2015. doi : 10.1002/ppap.201400162.

51. Meng B, Deng J, Liu Q, Wu Z, Yang W. Transparent and ductile poly (lactic acid)/poly (butyl acrylate)(PBA) blends: structure and properties. European Polymer Journal. 2012; 48(1):127-135. doi:10.1016/j.eurpolymj.2011.10.009.

52. Choudhury A, Bhowmick AK, Ong C. Novel role of polymer–solvent and clay–solvent interaction parameters on the thermal, mechanical and optical properties of polymer nanocomposites. Polymer. 2009; 50(1):201-210. doi:10.1016/j.polymer.2008.10.044.

53. Deng Y, Gu A, Fang Z. The effect of morphology on the optical properties of transparent epoxy/montmorillonite composites. Polymer International. 2004; 53(1):85-91. doi: 10.1002/pi.1410.

54. Petersson L, Oksman K. Biopolymer based nanocomposites: comparing layered silicates and microcrystalline cellulose as nanoreinforcement. Composites Science and Technology. 2006; 66(13):2187-2196. doi:10.1016/j.compscitech.2005.12.010.

55. Couderc P, Catherine Y. Structure and physical properties of plasma-grown amorphous hydrogenated carbon films. Thin Solid Films. 1987; 146(1):93-107. doi:10.1016/0040-6090(87)90343-9.

56. Tien PK, Smolinsky G, Martin RJ. Thin Organosilicon Films for Integrated Optics. Appl Opt. 1972; 11(3):637-642. doi: 10.1364/AO.11.000637.

57. Chatham H. Oxygen diffusion barrier properties of transparent oxide coatings on polymeric substrates. Surf Coat Technol. 1996; 78(1–3):1-9. doi:10.1016/0257-8972(95)02420-4.